Fabricating Polymer Solar Cells

John Knowles

***Abstract*—We determined a method of cleaning polymer LEDs during fabrication to improve device performance by removing contamination sources.**

We used a prepared 50mg solution of a polymer or a polymer blend and then transferred the finished solution into the spinning glove box in the center nitrogen-pumped ante chamber. We administered the polymer solution into two solvents, TFT and toluene, in order to dissolve the polymer.

We prepared a polymer layer and then wiped down excess solution to create a via between the electrodes. This was done to allow the cathode made of calcium to connect to the small ITO. Afterwards, we deposited a small amount of calcium to act as a conductive electrode. This was done in a vacuum, using a stencil in order to collect the deposited calcium in the desired regions.

We measured device characteristics and calculated associated efficiencies and fill-factors.

***Index Terms*—Bulk heterojunction organic photovoltaic cells, solar cells, photoelectric effect, substrate, polymers, P3HT, PCBM, ZZ50 (PCPDTBT), efficiency, fill-factor, Indium Tin-Oxide, Calcium,...**

I. Introduction

PHYS 422 is a polymer electronics lab that explores the production of bulk heterojunction organic photovoltaics.

A. Project Goals

To investigate the process of making Bulk Heterojunction Organic Photovoltaics (BHJs) so that better understanding of the current market technologies can be applied to future projects.

B. Motivation, Context and Justification

The future of energy requires a more affordable and cleaner solution that can possibly be realized through organic solar cells. If the manufacturing process can be reduced to a significant lack of complexity, either in the equipment needed to produce the completed substrates or through a novel method that can be done in the average garage, then the act of de-centralizing energy production would have significant impacts on energy conglomerates and their dependence of petroleum products.

The state of organic photovoltaic (OPV) cost production or power generation ability is not competitive with other established sources of energy production on the market. More research and experimentation is needed in order to reduce costs and inefficiencies of OPV production. I personally hold a desire to investigate the manufacturing process of organic solar cells with the intent of simplifying the process enough so that it can be considered "garage science."

Advisor: Professor Echols
Partner: Garret Heinan

Polymers have the potential to be cheaply manufactured, a clean, renewable source of energy, a fossil-fuel replacement, ultra-thin with high absorptivity, and printable.

C. Essentials of BHJ OPVs

BHJ diodes operate on the principle of the photovoltaic effect-which is the process of converting sunlight into electricity. Figure 1 shows a basic representation of how an OPV is constructed. Beginning with the glass substrate, an application

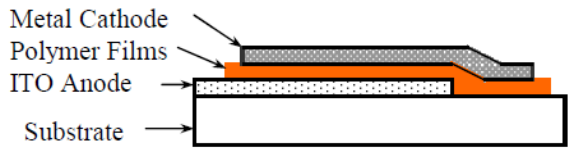

Fig. 1. Layered representation of an organic photovoltaic substrate.

of Indium Tin-Oxide (ITO) is prepared and functions as the anode of the device. The polymer film layer is the meat of the device, in which incident photons initiate the dynamics of current flow. Finally, the metal cathode is placed to complete the circuit.

The operational mechanism of current flow in OPVs can be generalized in a few steps, as shown below:

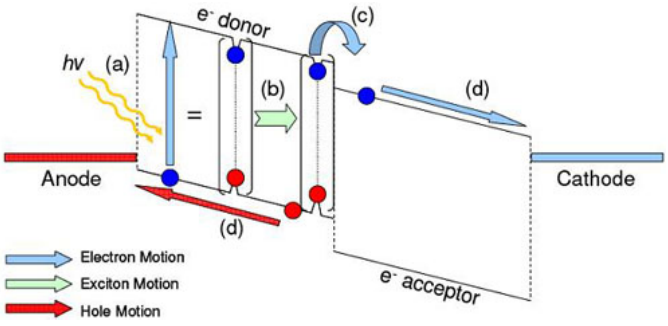

Fig. 2. Organic photovoltaic operational mechanisms are shown here. A visual emphasis on the inner-workings of the polymer film is beneficial towards understanding the physics of these solar cells.

a) The photon is absorbed in the active layer and produces an exciton.
b) The exciton diffuses along the polymer chain with a diffusion length of 10nm.
c) If there is donor/acceptor material interaction, then disassociation of the exciton occurs and charges are collected by the respective electrodes due to the internal electric field generated by differences in electrode work functions.
d) Current flow is established and an output voltage is collected.

II. Substrate Preparation

Since the glass substrate was already prepared with an ITO application, we began our journey with preparing the substrates for the application of PEDOT, a conducting polymer that planarizes the ITO surface, improves the hole injection from the ITO to the electroluminescent polymer (so excitons are easily made), and acts as a diffusion barrier to trap oxygen in the ITO.

Fig. 3. Cal Poly: SLO Polymer Electronics Lab. Featured (from left to right): Testing work station with labview , Measurement Equipment, Dolan Jenner MI-150 Spectrum Light Source, Evaporator (Aluminum or Calcium), Polymer application and wiping station, PEDOT application and wiping station, Dust-Free Hood, UV Ozone Reactor, Not featured: Fume Hood with ultrasonic bath, acetone and isoprophyl application, and nitrogen transport hose.

A. ACETONE & ISOPROPYL ALCOHOL BATHS

We performed an initial inspection of the substrate after cleaning hands with soap and water and equipped a lab coat, lab goggles, and dust-free gloves.

An ultrasonic bath increases the likelihood of removing contaminates from the substrate. This cleaning process was performed in the fume-hood so that there was no exposure to solvent vapors. We loaded the substrate holder and placed the collection into a closed-top beaker inside the fume-hood. This beaker contains acetone and it is placed inside the ultrasonic bath for a period of 3 minutes while the fume-sash is pulled down. Excess acetone is removed using a compressed nitrogen gun calibrated for low pressure use.

The collection of dry substrates were then placed into a beaker of isopropyl solution to remove leftover contaminants and covered. We repeated the process of cleaning the substrates inside the ultrasonic bath for three minutes inside the fume-hood.

A nitrogen gun was used to dry off the collection of substrates and also to transport the substrates from the fume-hood to the dust-free hood. A constant application of nitrogen incident on the substrate holder prevents the inclusion of contaminants by creating a pocket of nitrogen gas. We were careful to direct the nitrogen stream away from the dust-free hood.

B. UV OZONE REACTOR

An ultraviolet ozone process was used react with and disassociate organic components on the substrate. This process also possibly generates reactive atomic oxygen that cleans the substrate and may also diffuse into the ITO layer.

The Jelight ozone reactor door was opened and the substrates were placed at the back of the dust-free hood one at a time with the ITO side facing up. The goal was to provide a layer of ozone across the surface of each substrate. Once the substrates were placed, we closed the door to the Jelight ozone reactor and turned the UV light on for 15 minutes.

The cleaning process was concluded once the substrates were loaded back into the substrate holder and transported into the PEDOT application glovebox (See *PEDOT Application*.)

III. PEDOT Application

As previously stated, PEDOT is applied to the substrate for the following reasons:

- PEDOT is a conducting polymer that planarizes the ITO surface.
- It improves the hole injection from the ITO to the electroluminescent polymer (so excitons are easily made).
- and it acts as a diffusion barrier to trap oxygen in the ITO.

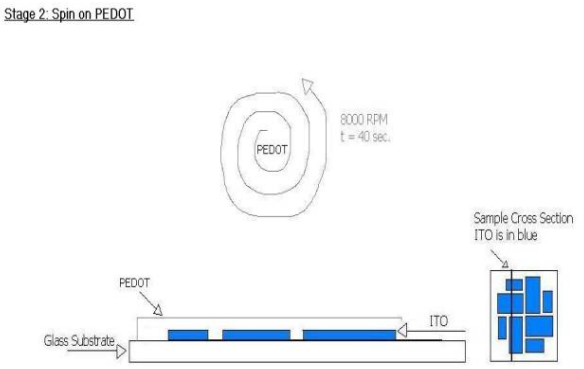

Fig. 4. PEDOT solution deposited onto the ITO side of the substrate

A prepared solution of PEDOT is applied by pipette to the ITO side of the substrate and then subsequently placed into a spin-coating device set for 8000 RPM for one minute. Once sufficiently coated, the substrate was placed onto a hot plate for 15 minutes with temperatures of 125 degrees Celsius to anneal the PEDOT of its solvent. Excess PEDOT was wiped from the edges of the substrate's small ITO pads (pads A and B) in order to reduce the chance of a short-circuit developing due to the PEDOT's conducting properties and it's arrangement between the electrodes.

IV. Preparation of the polymer solution

Polymer solutions were prepared beforehand, so there was no need to prepare the polymer solutions with their corresponding solvents.

The introduction of the active layer elements was either

a straight P3HT:PCBM application or a P3HT:ZZ50:PCBM blend. Each group was assigned polymer film assignments along with different spin speeds: 2k or 4k RPM. I was personally assigned a P3HT:ZZ50:PCBM blend spun at 4k RPM (with ITO pads A and B wiped of PEDOT.)

V. Spin Coating the Polymer Film

A half-millimeter of polymer solution was applied to the substrate and subsequently spun to create a thin layer.

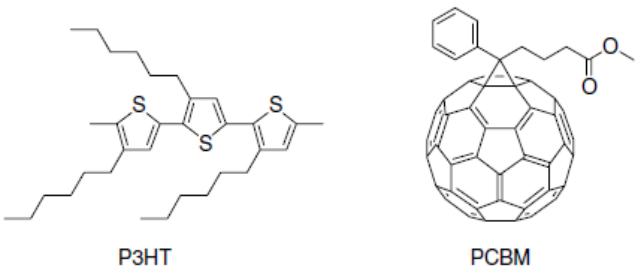

Fig. 5. P3HT and PCBM structures.

The process of spin-coating the P3HT:ZZ50:PCBM blend yielded some complications. Firstly, leftover solution was applied to the bottom of the substrate during the spin-coating process. This would have had significantly negative effects on the device functionality had the solution not been wiped. However, in the process of correcting the bottom of the glass substrate (the opposite side of the applied organic layers,) a mishap occurred and the substrate dropped into my glove. This

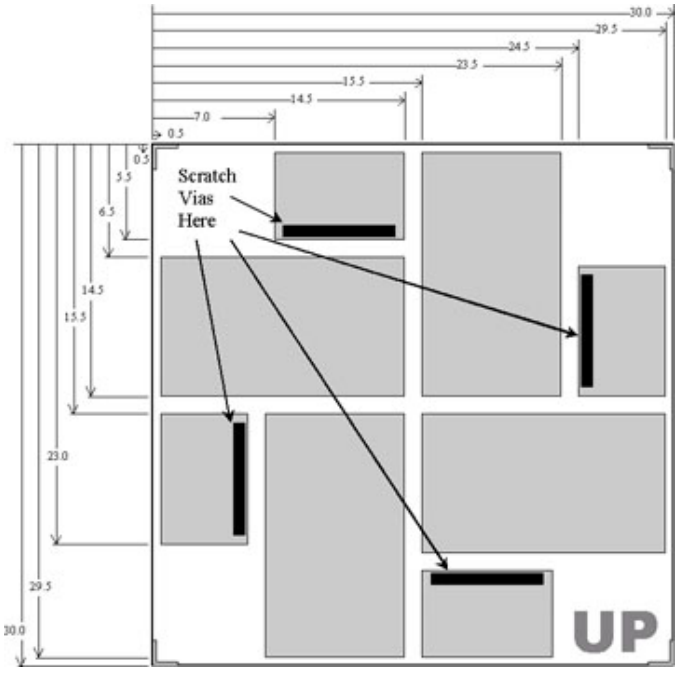

Fig. 6. Top-Down view of ITO pads and VIA locations.

mistake alone could have scratched the ITO pads significantly and introduced other contaminants. After picking the substrate back up, its position completely and unknowingly reversed, I proceeded to wipe half of the device in the process. ITO pads A and B were effectively shorted in this procedure. Despite this, I concluded this stage by creating VIAs for electrode contact by wiping the device of polymer film from the perimeter to the outside edge of the small ITO pads.

VI. Evaporation

We transferred the solar substrates to the vacuum chamber designated for the evaporation of the calcium cathode layer.

The calcium layer acts as an cathode and it is deposited onto the substrate using a vacuum evaporator. The vacuum evaporator sublimes the calcium in the process.

The evaporator setup is found inside the bell jar. Once the round shield, mask holder, and brace have been moved out of the way, the shutter and chimney are then moved out of the way.

Using tweezers, we removed excess calcium from the boat and then loaded a few new pieces of calcium into the boat. We used the vacuum to suck up any other excess calcium.

We replaced the chimney and the shutter and then put the brace back in place. Following that, the mask holder is returned to its prior location. We then vacuumed the mask holder and placed the ITO side of the substrate facing down in the mask holder.

The entire evaporation preparation is finished once the bell jar seal is vacuumed shut and clean, as well as the shield is placed back down on the apparatus.

We allowed the pressure gauge to read around 30 microns before closing the roughing valve, opening the fore line valve, and exposing a diffusion pump line. We waited for the TC gauge to read about zero before turning on the ionization gauge for the pressure to drop below 1.5x10÷6 Torr.

We flipped the variac power and turned the current slowly until the meter read 70Amps. After one minute, we opened the shutter and waited 5 minutes before increasing to 80 amps. Another five minutes before increasing to 90 amps. Five more minutes before turning the current down slowly and leaving the last 60 seconds to drop from 90 to 0. The final thickness of the calcium deposit was determined to be 439nm. We turned the power supply off and then prepared for testing.

VII. Testing

After the calcium was deposited, the initial testing of the devices were performed by Professor Echols. This data was to reflect the initial device performance characteristics soon after the calcium deposit was finished. The second round of measurements were performed after a week to observe the device's performance degradation as a function of time. A third round of measurements were taken after submitting the devices to a thermal anneal of 108 degrees Celsius. This annealing process was done to influence spinodal decomposition in the active layer.

Spinodal decomposition has been observed to positively impact the efficiencies and fill-factors of blended devices due to the fact that a thermal anneal causes P3HT to crystallize very well. It has also been observed to degrade the quality of PCBM and ZZ50 performance in the device at thermal

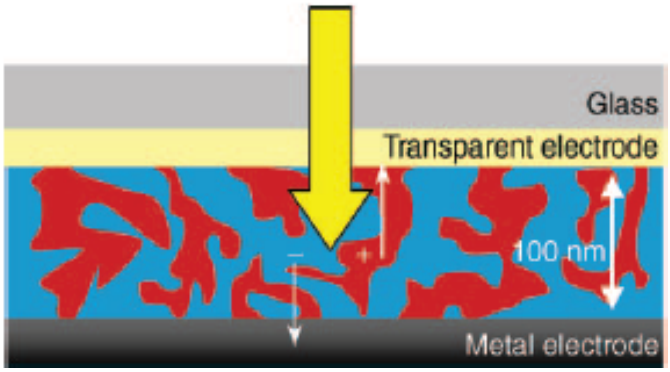

Fig. 7. A thermal anneal causes spinodal decomposition to occur in the polymer layer. Spinodal decomposition creates easier pathways for electron movement; therefore, better current flow.

anneal temperatures exceeding 150 degrees Celsius due to their amorphous qualities.

In the testing glovebox, we placed a substrate onto the test jig such that the glass layer was the upper-most layer and there was good electrode conduction with the 8 spring-loaded pins underneath the substrate.

We verified good pixel connections by applying 5V to each pixel housed and locked in by the aluminum plate. Then we ran an initial check in labview that gave us the sample substrate's device characteristics operating under 5V and 10A for the large pixels of 42mm$\hat{2}$. The smaller pixels have an area of 3.75mm$\hat{2}$, to which a relatively smaller current is needed in order to maintain the same current densities between both the large and small pixels.

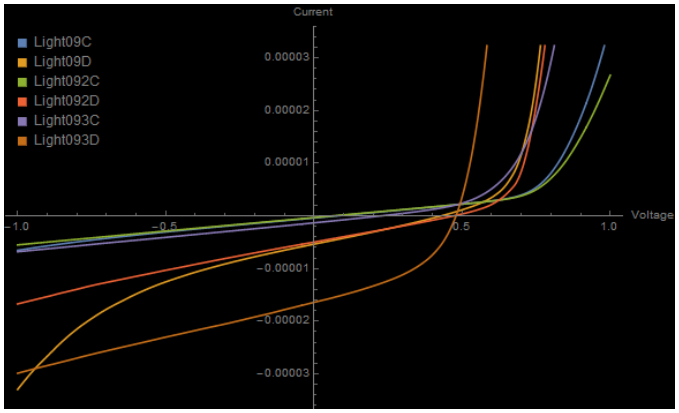

Fig. 8. Current vs. Voltage curves for each trial of measurements taken. ITO pads A and B were excluded since they were ultimately shorted. D1 to D3: reduced leakiness after thermal anneal.

A. Brightness and Efficiency

We applied a voltage difference and measure unit pixel current flow using a Keithley 236 Source Measure Unit or the Keithley 2400 Source Meter. The brightness of emitted light is measured with a photo-diode located in the testing jig. To calibrate and sample the photo-current, we either measured the photo-current directly using a Keithley 7514 electrometer.

In this case, we determine the brightness of the LED pixel to be the following:

$$LEDBrightness[\frac{cd}{m^2}] = PC * 405 * [\frac{cd}{m^2}]\frac{54[mm^2]}{LEDArea}$$

where PC is the photo-current and it is measured in μA and 1 μA of photo-current measured on the electrometer corresponds to 405 $[\frac{cd}{m^2}]$ for a $OC_1C_{10} - PPV$ device having an area of 54 $[mm^2]$.
Device efficiency was measured using the following:

$$Efficiency[\frac{lm}{A}] = \frac{PC[\mu A]}{current[A]}0.06[\frac{lm/A}{V/A}]$$

or

$$Efficiency[\frac{cd}{A}] = \frac{PC[\mu A]}{current[A]}0.06[\frac{lm/A}{V/A}] + \pi$$

or

$$Efficiency[\frac{lm}{W}] = \frac{PC[\mu A]}{current[A]} * 0.06[\frac{lm/A}{V/A}] \div V$$

Alternatively, we measure the photo-current indirectly by converting the photo-current into a photo-voltage using a transimpedence amplifier, followed by sampling the photo-voltage with a DMM.
The brightness of the LED pixel, noting that 1V of photo-voltage measured on the DMM corresponds to 2025$[\frac{cd}{m^2}]$ for a $OC_1C_{10} - PPV$ device with an area of 54 mm$\hat{2}$, is then found using the following equation:

$$LEDBrightness[\frac{cd}{m^2}] = PC[V] * 2025[\frac{cd}{m^2}][\frac{54mm^2}{LEDArea}]$$

to which the device efficiency was determined using

$$Efficiency[\frac{lm}{A}] = \frac{PC[V]}{Current[A]}0.03[\frac{lm/V}{V/A}]$$

or

$$Efficiency[\frac{cd}{A}] = \frac{PC[V]}{Current[A]}0.03[\frac{lm/V}{V/A}] + \pi$$

or

$$Efficiency[\frac{lm}{W}] = \frac{PC[V]}{Current[A]}0.03[\frac{lm/V}{V/A}] \div V$$

We finalized the testing process by obtaining luminance readings from the surrounding environment to determine associated errors.

VIII. Results

The results of our solar cells came out as expected. ITO pads A and B were wiped clean (and short-circuited.) The efficiency and fill-factor values are shown below:

Pixel	Efficiency (%)	Fill Factor
—	Day 1—Day 2—Day 3	Day 1—Day 2—Day 3
C (Small)	0.010—0.004—0.105	0.252—0.154—0.231
—	Day 1—Day 2—Day 3	Day 1—Day 2—Day 3
D (Big)	0.080—0.080—0.443	0.260—0.249—0.429

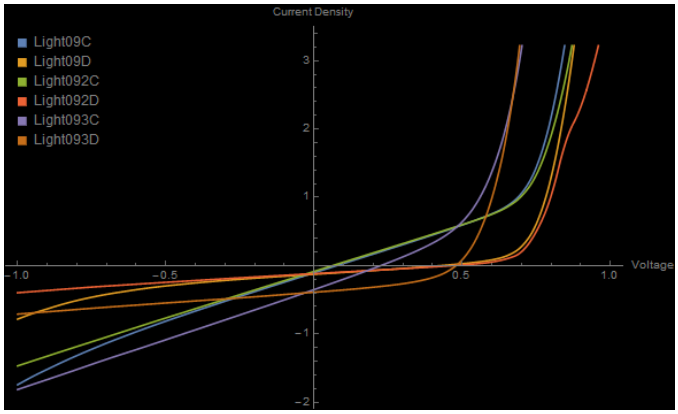

Fig. 9. Note the linearity of curves in the negative direction. With a thermal anneal, these curves changed from exponentially to linear. This observation shows a consideration of how leakiness is influenced by a thermal anneal. Small pixels are also more leaky

The results clearly show that efficiency and fill-factor of both pixels increased dramatically from Day 1 measurements to Day 3 measurements. Day 2 experimental data suggests that solar cell rest time had a negative impact on efficiencies and fill factors.

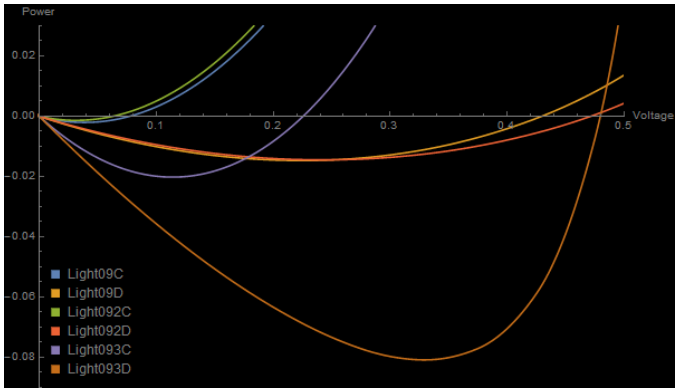

Fig. 10. Thermal anneal shows an increase in efficiency by factors of: C 10.25x and D 5.5x

IX. CONCLUSIONS

Group results were collaborated and the different experimental factors of each group were considered. For all of these results, it is difficult to say with certainty that any one factor or difference in experimental procedure yielded definite effects. Generally speaking, For higher spin speeds, an increase of efficiency and fill-factor values were recognized. Better performance characteristics were recognized for the blended devices, i.e.: P3HT:ZZ50:PCBM blends. The additional two devices that were created without PEDOT layers did not seem to influence much. My device was the only one in class that had an applied PEDOT layer that had not been wiped on the active small ITO pad.

Ideally, I would like to repeat this experiment with better controls and a lot more tinkering around with different organic materials.

REFERENCES

[1] Berland, Brian. Photovoltaic Technologies beyond the Horizon: Optical Rectenna Solar Cell. Final Report, NREL/SR-520-33263, 2003. http://www.nrel.gov/docs/fy03osti/33263.pdf.
[2] Brabec, Christoph J., and James R. Durrant. Solution-Processed Organic Solar Cells. Mrs Bulletin 33, no. 7 (2008): 670675.
[3] Braun, David. A Senior Level Polymer Electronics Course: Unique Instruction or Just Low Cost? Electrical Engineering, 2005, 39.
[4] D. Braun, http://www.ee.calpoly.edu/ dbraun/polyelec/, accessed 2016
[5] D. Braun, http://www.ee.calpoly.edu/ dbraun/polyelec/moreinfo.html, accessed 2016
[6] Janssen, Ren AJ, Jan C. Hummelen, and N. Serdar Sariciftci. Polymerfullerene Bulk Heterojunction Solar Cells. MRS Bulletin 30, no. 1 (2005): 3336.
[7] Herrick, Spencer. Organic Polymer Solar Cells: The Effects of Device Packaging on Cell Lifetime, 2013. http://digitalcommons.calpoly.edu/physsp/78/.
[8] Olson, Grant. Multipolymer Interactions in Bulk Heterojunction Photovoltaic Devices, 2012. http://digitalcommons.calpoly.edu/physsp/59/.